Effect of Strand Damage in Nb_3Sn Rutherford Cables on the Quench Propagation in Accelerator Magnets

R. Keijzer, G. Willering, M. M. J. Dhallé, and H. H. J. ten Kate

***Abstract*—Accelerator magnets employing Nb_3Sn Rutherford cables are more susceptible to conductor degradation than Nb-Ti magnets. Recent measurements on a Nb_3Sn accelerator magnet have revealed unexpected behaviour such as decaying voltages at constant current plateaus of V-I measurements, inverse ramp rate and temperature dependence of quench currents, and anomalous quench propagation measured by so-called quench antennas. Numerical modelling has shown that these anomalies can be explained by an inhomogeneous degradation in the Rutherford cable, in which a subset of strands is fully or partially degraded. In this paper, we study how this type of degradation can affect the early stages of quench propagation. With the aid of a network model, we show how quench antenna signals can be used to diagnose inhomogeneous conductor degradation in the Rutherford cable.**

***Index Terms*—Accelerator magnets, Nb_3Sn, Rutherford cable, Quench.**

I. Introduction

In RECENT years, several new 11 T class accelerator magnets employing Nb_3Sn technology have been tested at the superconducting magnet test facility at CERN [1]. This test campaign has revealed the challenges inherent to the use of Nb_3Sn, which is more prone to conductor degradation than Nb-Ti. The reduced performance of these magnets was accompanied by anomalous measurement signals captured by several diagnostic tools. These anomalous signals include decaying voltages on the current plateaus of V-I measurements, inverse ramp-rate and temperature dependence of quench current, and anomalous quench propagation observed with quench antennas.

For a better understanding of the nature of the degradation in the Nb_3Sn Rutherford-type cables, studies are done into the physical mechanisms behind these anomalous measurements. Previously the anomalous V-I measurement were studied [2], [3]. In this work, the focus is on the interpretation of quench antenna signals captured from an 11 T magnet, MBHA002 [4].

Fig. 1(a) shows the lay-out of a local quench antenna system placed in a magnet bore [5]. In the transverse plane each quadrant contains one pick-up coil. To compensate for noise generated by the main field component the coils are paired up in series, with coil C connected to A and D connected to B. The pick-up coils of the quench antenna are arranged in an array of individual elements that have an axial length of 40 mm and an azimuthal width of 10 mm, as shown in Fig. 1(b), where only 5 of the 11 C-coils are shown.

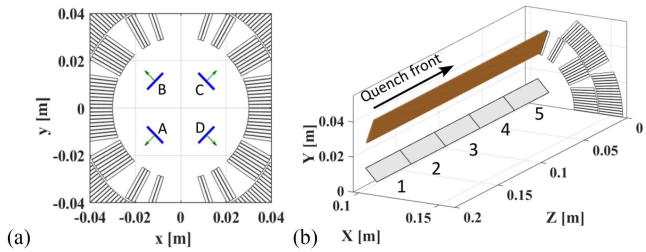

Fig. 1. (a) Cross-section of an 11 T dipole magnet showing the location and polarity of the pick-up coils in the transverse plane. (b) Five of the eleven pick-up coils are shown in their position along with Rutherford cable in the pole turn. A quench front passing by these pick-up coils results in an inductive signal.

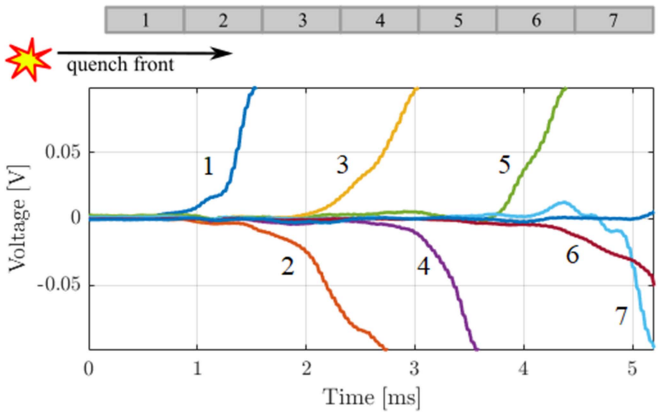

Fig. 2. Voltage signals acquired by the coil combination C+A during the measurements. The quench starts in front of the quench antenna array after which the quench front moves past the different pick-up coils. In each consecutive pick-up loop the sign of the signal changes, except for the last two. Note that the signal saturates at 0.1 V, the signal after saturation is not shown here.

In Fig. 2 the anomalous quench antenna signals are shown acquired by the coil combination C+A. The magnet quenched at 11.6 kA at an operation temperature of 4.5 K. The signal in the pick-up coils is induced by the field changes due to current redistribution in the cable. In this case, the signal alternates sign as the quench front propagates alongside the different pick-up

Manuscript received 13 November 2022; revised 22 January 2023; accepted 24 January 2023. Date of publication 14 February 2023; date of current version 21 February 2023. *(Corresponding author: Ruben Keijzer.)*

R. Keijzer is with the CERN, CH1211 Geneva, Switzerland, and also with the University of Twente, 7522 NB Enschede, The Netherlands (e-mail: ruben.keijzer@cern.ch).

G. Willering is with the CERN, CH 1211 Geneva, Switzerland.

M. M. J. Dhallé and H. H. J. ten Kate are with the University of Twente, 7522 NB Enschede, The Netherlands.

Color versions of one or more figures in this article are available at https://doi.org/10.1109/TASC.2023.3244140.

Digital Object Identifier 10.1109/TASC.2023.3244140

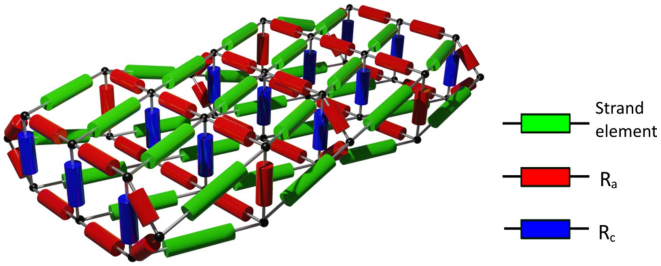

Fig. 3. Network model of a Rutherford cable consisting of 8 strands. The strand elements are modelled as two parallel resistors representing the copper matrix and the superconductor.

TABLE I
CABLE PARAMETERS FOR SIMULATION

Parameter	Value
R_a/R_c	0.5/200 μΩ
α	0.2 W/m/K^{1+b}
b	1.54
Cable twist pitch	0.1 m
Number of strands	40
Cable width	15 mm
Strand diameter	0.7 mm
Copper non-copper ratio	1.15
Copper RRR	100
I_c@1.9K/12T	585 A

coils. This behavior is not compatible with our current understanding of quench propagation. According to present models one would expect each pick-up coil in the array to acquire a signal with the same sign when the quench front passes by [5], [6].

Previously, a simulation study concluded that anomalous V-I measurements observed on this same magnet are likely caused by the presence of a local inhomogeneous degradation of the conductor that results in a large current imbalance in the Rutherford cable [3]. The current redistributes around the defect in such a way that the adjacent strands take up all the excess current [2], [3]. In this work, we study whether this current imbalance can also explain the anomalous quench propagation observed by the local quench antenna system. To this end, a numerical thermal-electric network model is used to simulate the quench development of a Rutherford cable with different initial current distributions.

In Section II we explain the model, in Section III we present the simulation results, in Section IV we discuss them, followed by the conclusion in Section V.

II. NETWORK MODEL

Several models have been used to study the quench behavior of Rutherford-type cable structures in the past. Notably, the CUDI model has been used to study their thermal stability [7], [8], [9] and the THELMA model was used to study quench propagation [10], [11].

Here, we use a newly developed coupled thermal-electric network model using a similar modelling philosophy as CUDI, but with a different network layout employing fast numerical solvers [12], [13]. The solver employs soft-coupling between the electric and thermal sub-domains.

The electric domain is treated with a network analysis, the electrical network is depicted in Fig. 3. Each strand element is modelled with a current sharing model, where the copper is treated as a temperature and magnetic field dependent resistor and the Nb_3Sn superconductor is modelled with a power-law. The self and mutual inductances between elements are calculated using the expressions from [14]. The scaling laws for the critical surface of Nb_3Sn are taken from the ITER parametrization [15]. The adjacent and crossing electrical inter-strand contact resistances, respectively R_a and R_c, are assumed to be constant, the values are taken from [9].

The boundary conditions impose a fixed current and are placed sufficiently far away as to not influence the quench process, this requirement leads to a modelled length of 0.5 m.

The thermal domain is modelled with a lumped element approach. It is assumed that each element has a homogeneous temperature throughout its cross-section. The thermal inter-strand contact conductance is calculated with a temperature dependent empirical relation from literature [18], [19], [20]:

$$k = \alpha T^b [\mathrm{W/m/K}] \tag{1}$$

Unless stated otherwise, the model parameters are as listed in Table I. The thermal and electric material properties are taken from [17]. The field gradient in the cable is calculated with ROXIE, where it is assumed that the quench occurs in the pole turn of the magnet [12]. During each time step the contribution of the cable self-field is updated.

Quench simulations depend on a number of empirical material parameters that are subject to a significant degree of uncertainty, notably the inter-strand contact parameters. Heat treatment details, pre-stress, and surface oxidation, among others, all affect these parameters. For this reason, measurements on cable samples may not be representative if even one of these factors is different. Therefore, also a sensitivity analysis was done to understand the cable behavior within physically meaningful limits.

The results of the quench simulation are then used to calculate the rate-of-change of the flux linkages in the quench antenna segments with a Biot-Savart-type of integral. The field is evaluated at the center points of a 20x10 grid on the surface spanned by the pick-up coils.

III. RESULTS

A. Quench With a Homogeneous Current Distribution

First, we study the quench behavior of a Rutherford cable with a homogeneous initial current distribution, all strands carry the same current. All simulations are done with a cable current of 11.6 kA at a temperature of 4.5 K. In Fig. 4 the current evolution is shown as a 2D color plot providing a 'top view' of the 3D Rutherford cable model. The quench is initiated with a small heat pulse at the high-field edge of the cable. After all strands have quenched in the transverse direction the quench front propagates longitudinally in a uniform manner. Note that the gradient in the

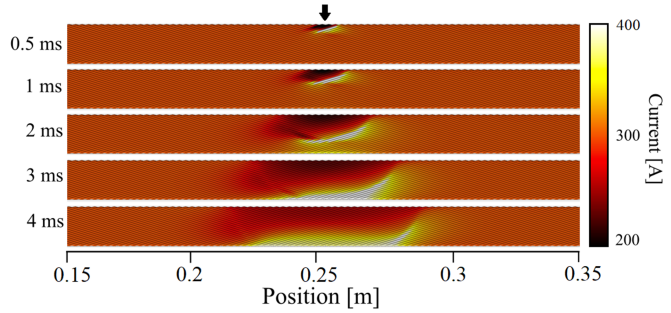

Fig. 4. 2D plots of the current evolution in the plane of Rutherford cable during a quench with a homogeneous initial current distribution. The quench is initiated at the cable edge marked by the arrow.

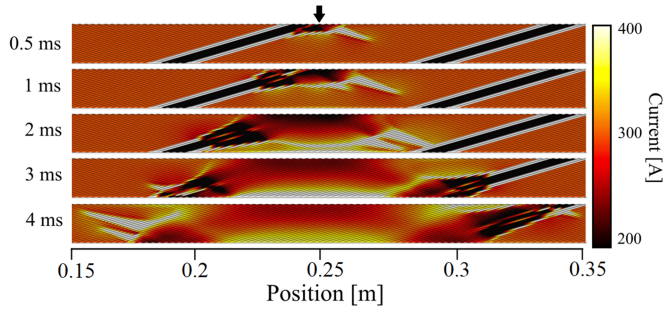

Fig. 6. Quench front for the inhomogeneous case. The longitudinal QPV of an overloaded strand is much greater than the transverse QPV between strands. Therefore, the overloaded strands lead the quench front, followed by a 'wake' of quenching strands.

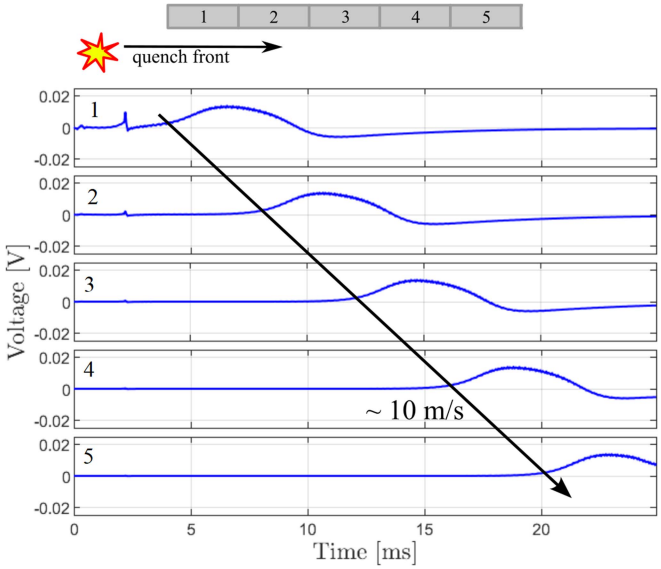

Fig. 5. Voltage signals from pick-up coils in quench antenna array for the homogeneous case. The quench starts in a location before the quench antenna array. The small spike at 2 ms is caused by the culmination of the quench in the transverse direction. As the quench front approaches the first pick-up coil (top-graph) its voltage starts to rise at 4 ms. The same voltage rise is seen in the other coils (graphs below) at a later time indicating the passing quench front. Note also that the voltage becomes negative as the quench front moves away.

current level over the cable width is caused by the magneto-resistivity of the copper.

The calculated quench antenna signals are shown in Fig. 5. The propagating quench front is registered by successive pick-up coils with the voltage rise having the same sign for each pick-up loop, as is expected for a fully developed quench front. The quench propagation velocity in this case is about 10 m/s.

B. Quench With an Inhomogeneous Current Distribution

Next, we study how an inhomogeneous current distribution in the Rutherford cable affects these results. From V-I measurements we have a strong indication that an inhomogeneous current distribution is present at the quench onset [2]. From simulation studies we know that in case of a homogeneous defect the adjacent strands take up the excess current [2], [3]. Once these strands reach their critical current, they are saturated, and the next adjacent strands takes up the excess current. For the simulation we opt for a current distribution where two strands are in the saturated state on either side of the defect. This current distribution is imposed as the initial condition of the model. In the conductors of an actual magnet this current distribution may be expected to vary in space, but since only a few twist pitches are considered in the model it is kept constant here. This state is denoted as the inhomogeneous case.

In Fig. 6, the current evolution with time is shown for this case. The inhomogeneous current distribution is visible from the start. The quench front looks markedly different from the homogeneous case presented in Fig. 4. The overloaded strands are leading the quench front followed by a gradually expanding 'wake' of quenching strands. For a correct prediction of the quench propagation velocity, it is no longer possible to treat the cable as a homogenized entity, as often done in quench propagation velocity calculations [21], [22]. Instead, thermal and electrical inter-strand contact resistances will play a significant role.

In Fig. 7 the corresponding voltage signals of the quench antenna array are shown. In this case, the passing of the quench front is not as well-defined as it was in the homogeneous case. The sign of the signal changes for several consecutive quench antennas, as also observed in actual measurements (Fig. 2). Moreover, the quench propagation velocity has increased significantly to about 29 m/s.

C. Parametric Studies

A sensitivity analysis involving the electrical and thermal inter-strand contact conductance is carried out to study how they influence the quench propagation under inhomogeneous conditions. In Fig. 8, the quench propagation velocity (QPV) is shown as a function of R_a for different numbers of saturated strands. In this case, we fix the value of α (the scaling factor for the thermal conductance) at 0.2 W/m/K^{1+b}.

The quench propagation velocity is higher for lower values of R_a. In case of one saturated strand the QPV matches the homogeneous case for R_a values greater than 7 $\mu\Omega$, this does not happen with two or more saturated strands. The QPV is affected this way because the length scale of electrical diffusion increases

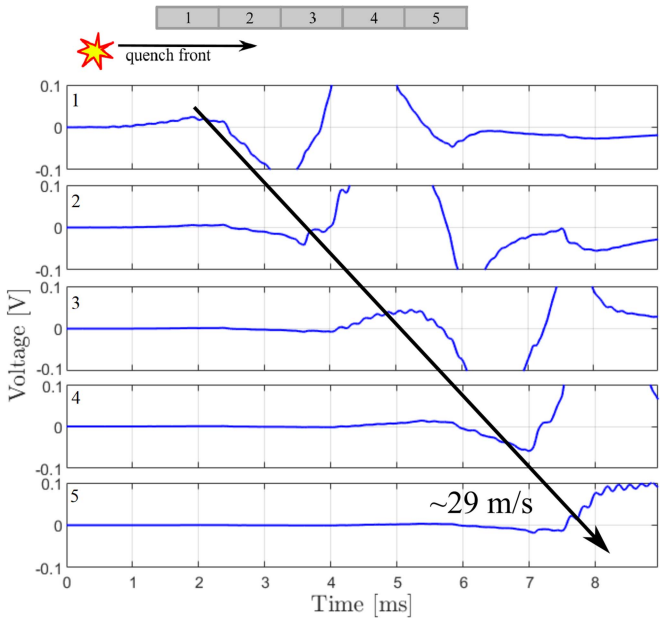

Fig. 7. Voltage signals from pick-up coils in quench antenna array for the inhomogeneous case. In this case the quench front is less well defined, the signal shapes differ between pick-up coils, and the sign of the signal changes between consecutive pick-up coils. The signal amplitude is also much larger than in the homogeneous case.

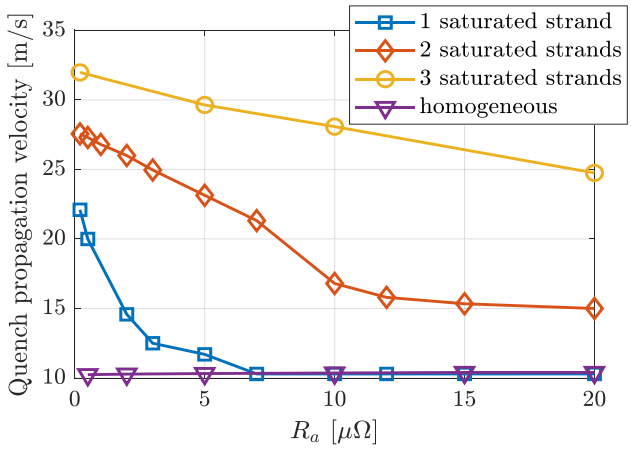

Fig. 8. Quench propagation velocity as a function of R_a for different numbers of saturated strands. α is kept constant at 0.2 W/m/K^{1+b}.

with an increasing R_a. The electrical current redistribution from the overloaded strand into the neighboring strands then precedes the thermal quench front. Consequently, for a higher R_a more of the current will already have flown out of the saturated strand when the thermal quench front reaches a certain part of the strand resulting in a lower QPV. The QPV for the homogeneous case is not affected by the value of R_a.

A similar study is done for the thermal inter-strand contact parameter α. All other parameters are kept as they are in Table I. The results are shown in Fig. 9. For the homogeneous case we again see no relation between the QPV and the thermal contact resistance. With one saturated strand, there seems to

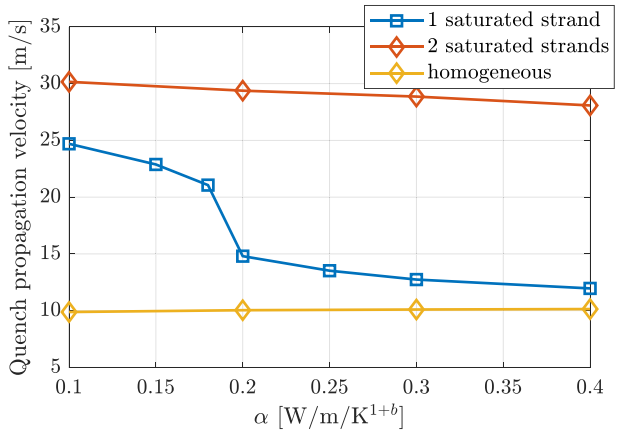

Fig. 9. Quench propagation velocity as a function of α for different numbers of saturated strands. R_a is kept constant at 1 $\mu\Omega$ for each simulation.

be two regimes with a sudden transition between them around 0.18 W/m/K^{1+b}. This transition is no longer present when two or more strands are saturated.

It should be noted that the quench propagation velocity is not constant in the non-homogeneous case. Due to the twist pitch the quench front in the saturated strand(s) will eventually move into the low-field part of the cable. Here the quench will slow down due to the larger thermal margin, and the other strands might even catch up depending on the inter-strand contact resistances.

IV. Discussion

Qualitatively, the anomalous behavior of the quench antenna signals can be explained reasonably well. However, quantitatively, the simulated quench propagation velocity remains well below the measured value of about 55 m/s. This quantitative discrepancy between model and experimental data may be caused by some assumptions in the model. In particular, it is assumed that a strand element has a homogeneous temperature throughout the strand's cross-section. For the high current densities that are present in the saturated strands the time constants may be too short for this assumption to be valid. It has been noted on the past that treating the strand elements in a homogenized way may not be accurate in certain strand stability regimes [9], [23]. The copper in-between the embedded Nb_3Sn filaments may have to be modelled as separate entity from the rest of the copper. This could result in the strand quenching much faster than is predicted with the assumptions made in this study.

V. Conclusion

Anomalous quench antenna signals observed in Nb_3Sn accelerator magnets have been investigated with a simulation study using a thermal-electric network model. The unexpected behavior can be explained by the presence of degraded strands and a resulting inhomogeneous current distribution at quench onset. The overloaded strands quench much faster than the other strands, which causes a non-uniform quench front and an increased quench propagation velocity.

These model predictions are compatible with the results of a previously conducted study of anomalous V-I measurements from the same magnet, where such a current distribution caused by a local inhomogeneous degradation was also shown to be the likely cause of the unexpected voltage signals.

On a more general note, we conclude that local quench antennas are thus a useful tool to detect the presence of such inhomogeneous current distributions present before the quench and can serve as an important performance indicator.

REFERENCES

[1] F. Savary et al., "Progress on the development for the Nb_3Sn 11T dipole for the high luminosity upgrade of the LHC," *IEEE Trans. Appl. Supercond.*, vol. 27, no. 4, Jun. 2017, Art. no. 4003505.

[2] G. Succi, L. Bottura, and M. Breschi, "On the effect of strand breakage on the operating margin of a Nb_3Sn Rutherford cable," *Cryogenics*, vol. 125, 2022, Art. no. 103458.

[3] R. Keijzer et al., "Modelling V-I measurements of Nb_3Sn accelerator magnets with conductor degradation," *IEEE Trans. Appl. Supercond.*, vol. 32, no. 6, Sep. 2022, Art. no. 4001105.

[4] G. Willering, "MBHA002 final test report," 2021. Accessed: Sep. 12, 2022. [Online]. Available: https://edms.cern.ch/document/2611118/1

[5] M. Calvi, E. Floch, S. Kouzue, and A. Siemko, "Improved quench localization and quench propagation velocity measurements in the LHC superconducting dipole magnets," *IEEE Trans. Appl. Supercond.*, vol. 15, no. 2, pp. 1209–1212, Jun. 2005.

[6] M. Marchevsky et al., "Magnetic detection of quenches in high-field accelerator magnets," *IEEE Trans. Appl. Supercond.*, vol. 23, no. 3, Jun. 2013, Art. no. 9001005.

[7] A.P. Verweij, "CUDI: A model for calculation of electrodynamic and thermal behaviour of superconducting Rutherford cables," *Cryogenics*, vol. 46, no. 7–8, pp. 619–626, 2006.

[8] G. Willering, "Stability of superconducting Rutherford cables for accelerator magnets," Ph.D. dissertation, Low Temperature Div., Univ. Twente, Enschede, The Netherlands, 2009.

[9] W. M. de Rapper, "Thermal stability of Nb_3Sn Rutherford cables for accelerator magnets," Ph.D. dissertation, Low Temperature Div., Univ. Twente, Enschede, The Netherlands, 2014.

[10] G. Manfreda and F. Bellina, "Analysis of the quench propagation along Nb_3Sn Rutherford cables with the THELMA code. Part I: Geometric and thermal models," *Cryogenics*, vol. 80, no. Part 3, pp. 357–363, 2016.

[11] G. Manfreda, F. Bellina, H. Bajas, and J.C. Perez, "Analysis of the quench propagation along Nb_3Sn Rutherford cables with the THELMA code. Part II: Model predictions and comparison with experimental results," *Cryogenics*, vol. 80, no. Part 3, pp. 364–373, 2016.

[12] C. Rackauckas and Q. Nie, "DifferentialEquations.jl–a performant and feature-rich ecosystem for solving differential equations in Julia," *J. Open Res. Softw.*, vol. 5, no. 1, 2017, Art. no. 15.

[13] A.C. Hindmarsh et al., "SUNDIALS: Suite of nonlinear and differential/algebraic equation solvers," *ACM Trans. Math. Softw.*, vol. 31, no. 3, pp. 363–396, 2005.

[14] F. W. Grover, *Inductance Calculations—Working Formulas and Tables*. New York, NY, USA: Dover Publications, 1946, pp. 55–58.

[15] L. Bottura and B. Bordini, "$J_c(B,T,\varepsilon)$ Parametrization for the ITER Nb_3Sn production," *IEEE Trans. Appl. Supercond.*, vol. 19, no. 3, pp. 1521–1524, Jun. 2009.

[16] G. Manfreda, "Review of ROXIE's material properties database for quench simulation," Accessed: Jun. 6, 2022, CERN Internal Note 2011-24. [Online] Available: https://edms.cern.ch/document/1178007/2

[17] S. Russenschuck, "Proceedings of the first international ROXIE users meeting," CERN report 99-01, Geneva, 1999.

[18] L.J. Salerno and P. Kittel, "Thermal contact conductance," Technical memorandum, 110429, NASA, Ames Research Center, Moffett Field, CA, USA, Feb. 1997.

[19] M. J. Nilles and S. W. van Sciver, "Effects of oxidation and roughness on Cu contact resistance from 4 to 290 K," *Adv. Cryogenic Eng.*, vol. 34, pp. 443–450, 1988.

[20] Y. Lei et al., "Measurements of interstrand thermal and electrical conductance in multistrand superconducting cables," *IEEE Trans. Appl. Supercond.*, vol. 12, no. 1, pp. 1052–1055, Mar. 2002.

[21] M. Wilson, *Superconducting Magnets*. Oxford, U.K.: Oxford Univ. Press, 1983, pp. 204–208.

[22] L. Dresner, *Stability of Superconductors, Selected Topics in Superconductivity*. New York, NY, USA: Springer, 1995, pp. 83–93.

[23] M. Breschi et al., "Comparing the thermal stability of NbTi and Nb_3Sn wires," *Supercond. Sci. Technol.*, vol. 22, 2009, Art. no. 25019.